THE JOURNAL OF COMPARATIVE NEUROLOGY 498:180–193 (2006)

Reevaluation of *Drosophila melanogaster's* Neuronal Circadian Pacemakers Reveals New Neuronal Classes

ORIE THOMAS SHAFER,[1] CHARLOTTE HELFRICH-FÖRSTER,[2] SUSAN CHRISTINE PORTIA RENN,[1] AND PAUL H. TAGHERT[1]*
[1]Department of Anatomy and Neurobiology, Washington University School of Medicine, St. Louis, Missouri 63110
[2]Universität Regensburg, Institut für Zoologie, Lehrstuhl für Entwicklungsbiologie, 93040 Regensburg, Germany

ABSTRACT

In the brain of the fly *Drosophila melanogaster,* ~150 clock-neurons are organized to synchronize and maintain behavioral rhythms, but the physiological and neurochemical bases of their interactions are largely unknown. Here we reevaluate the cellular properties of these pacemakers by application of a novel genetic reporter and several phenotypic markers. First, we describe an enhancer trap marker called R32 that specifically reveals several previously undescribed aspects of the fly's central neuronal pacemakers. We find evidence for a previously unappreciated class of neuronal pacemakers, the lateral posterior neurons (LPNs), and establish anatomical, molecular, and developmental criteria to establish a subclass within the dorsal neuron 1 (DN1) group of pacemakers. Furthermore, we show that the neuropeptide IPNamide is specifically expressed by this DN1 subclass. These observations implicate IPNamide as a second candidate circadian transmitter in the *Drosophila* brain. Finally, we present molecular and anatomical evidence for unrecognized phenotypic diversity within each of four established classes of clock neurons. J. Comp. Neurol. 498: 180–193, 2006.

Indexing terms: ***Drosophila*; circadian clock; neuropeptides; PDF receptor; IPNamide; *nplp1; glass***

Overt biological rhythms such as the predictable daily leaf movements of plants and the sleep/wake cycle of animals are ultimately driven by molecular oscillations. Throughout the living world such oscillations are sustained by intracellular transcriptional/translational feedback loops (reviewed by Dunlap, 1999). In *Drosophila* many components of the molecular clock are known in detail. Products of the clock genes *period (per), timeless (tim), Clock, cycle, vrille*, and *PAR domain protein 1 (Pdp1)* form two interconnected and self-sustained transcriptional feedback loops, the kinetics of which are regulated by clock protein interactions and attendant kinases (recently reviewed by Hardin, 2004; Schöning and Staiger, 2005; Taghert and Lin, 2005). Although the core clock genes are expressed rhythmically throughout the fly's body, only a few small groups of clock-expressing neurons in the central brain (termed pacemakers) are necessary and sufficient for the organization and maintenance of rhythmic locomotor activity (reviewed by Hall, 2005; Helfrich-Förster, 2005). When these pacemaker neurons of *Drosophila* are electrically silenced their molecular os-

Grant sponsors: Washington University Medical School (Keck Fellowship and NIH Vision Training Grant to O.T.S.); Grant sponsor: National Institutes of Health (NIH); Grant number: MH067122 (to P.H.T.); Grant sponsor: Deutsche Forschungs Gemeinschaft; Grant number: Fo207-9-1 (to C.H.-F.).

Current address for S.C.P. Renn: Bauer Center for Genomics Research, Harvard University, 7 Divinity Ave., Rm. 249, Cambridge, MA 02138.

*Correspondence to: Paul Taghert, Dept. Anatomy and Neurobiology, Washington University School of Medicine, 660 S. Euclid Ave., St. Louis, MO 63110. E-mail: taghertp@pcg.wustl.edu

Received 9 September 2005; Revised 16 December 2005; Accepted 9 March 2006

DOI 10.1002/cne.21021

Published online in Wiley InterScience (www.interscience.wiley.com).

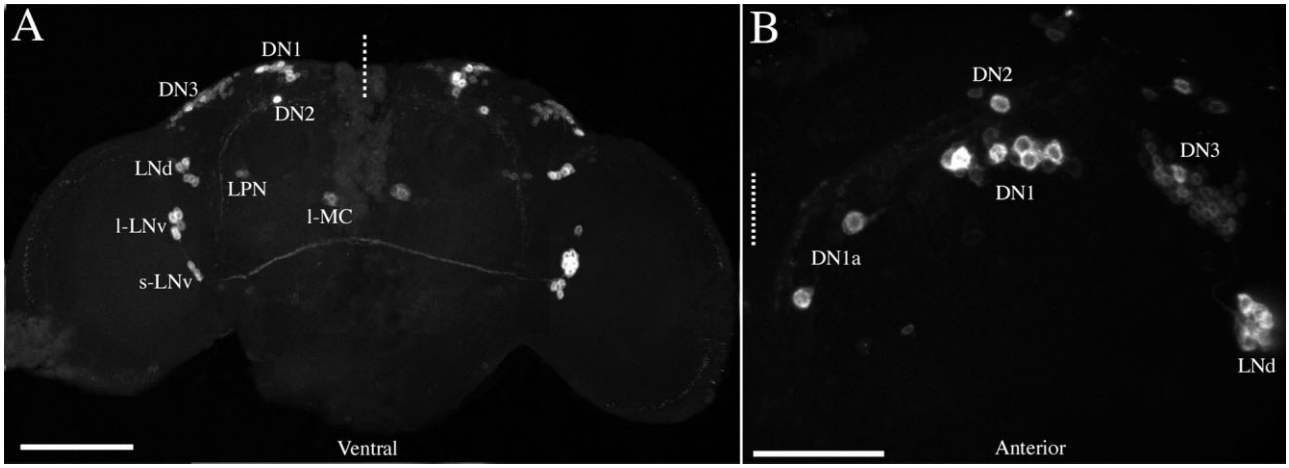

Fig. 1. R32-mediated LacZ expression in the adult brain. **A:** A projected Z-series montage of an adult R32 brain labeled for LacZ and imaged through its posterior surface. Cell classes are labeled in the left hemisphere. The dashed line represents the midline and the ventral aspect is labeled. Z-series depth was 150 μm. **B:** A projected Z-series through a single hemisphere of the dorsal protocerebrum, imaged through the dorsal surface. Two $DN1_a$s were clearly discernable in this orientation. The dashed line indicates the midline and the anterior aspect is labeled. Z-series depth was 80 μm. Scale bars = 100 μm in A; 20 μm in B.

cillations are lost under constant conditions, suggesting that electrical activity at the cell membrane is required for the endogenous molecular clockwork (Nitabach et al., 2002).

Approximately 150 neurons express the dynamic molecular clockwork in the adult brain and are divided into six groups based on location and size (Ewer et al., 1992; Frisch et al., 1994; Kaneko and Hall, 2000; Helfrich-Förster, 2003) (Fig. 1A). These are the large and small ventrolateral neurons (the l-LN_vs and s-LN_vs, respectively), the dorsolateral neurons (LN_ds), and three groups of dorsal neurons (DNs), the DN1s, DN2s, and DN3s. All six neuronal classes have been recognized for more than a decade (Ewer et al., 1992; Frisch et al., 1994) and no new classes of clock-neurons (i.e., neurons that support clock-gene oscillations under light:dark cycles or constant conditions) have been described in the central brain since that time (Hall, 2005). Hundreds more glial cells express clock products throughout the brain (Ewer et al., 1992), although the details of the molecular oscillations within glia and their role in directing behavioral rhythms is currently undefined.

The extent to which locomotor rhythms require specific neuronal classes has been investigated by the targeted deletion of clock neuron classes or the specific rescue of clock function within them (reviewed by Hall, 2005; Helfrich-Förster, 2005). The LN_v and LN_d are necessary and sufficient for the maintenance of locomotor rhythms in the absence of environmental times cues (Frisch et al., 1994; Helfrich-Förster, 1998; Renn et al., 1999) and for normal crepuscular organization of locomotion under light:dark (LD) conditions (Renn et al., 1999). Recent mosaic analysis suggests that the morning peak of activity is controlled by the s-LN_v, while the evening peak is governed by a group of neurons that include the LN_d and a subset of the DN1s (Stoleru et al., 2004; Grima et al., 2004). The specific functions of the l-LN_vs are not known. DNs are not required for locomotor rhythms under constant darkness (DD) and temperature, but contribute to the organization and/or entrainment of such behavior under LD conditions (Veleri et al., 2003; Klarsfeld et al., 2004).

Notwithstanding the ability to assign functions to most classes of clock neurons, the physiological and synaptic basis of these functions is poorly understood. For example, only one neurochemical output has been identified for clock neurons, a neuropeptide called pigment dispersing factor (PDF). PDF is expressed in both the large and small LN_vs and is required for the maintenance of locomotor rhythms under constant conditions and the normal timing of locomotion under LD (Renn et al., 1999). The transmitter phenotypes of the remaining clock-neuron classes remain a mystery, as do the synaptic interactions that organize neuronal timekeeping.

To provide ongoing studies of circadian pacemaker networks with greater cellular resolution, we reanalyzed the identities, anatomical position, and cellular properties of the clock neurons in the fly. In the present study we employ the detection of a local enhancer by a LacZ inser-

Abbreviations

DN1	Dorsal neuron group 1
$DN1_a$	Anterior dorsal neuron group 1
$DN1_p$	Posterior dorsal neuron group 1
DN2	Dorsal neuron group 2
DN3	Dorsal neuron group 3
dp	Dorsal projection of the s-LN_v
GFP	Green fluorescent protein
IPNa	IPNamide
LacZ	β-galactosidase
l-LN_v	Large ventral lateral neuron
l-MC	Large medial cell
LN_v	Ventral lateral neuron
LN_d	Dorsal lateral neuron
LPN	Lateral posterior neuron
PDF	Pigment dispersing factor
PDP1	PAR domain protein 1
PER	Period
pot	Posterior optic tract
TIM	Timeless

tion called P{wF6-84,R32} ("R32"; Schneider et al., 1993) to describe the clock-neuron classes of *Drosophila*'s central brain. First, we show that R32 is a limited and highly accurate reporter for neuronal PER in the adult brain. Next we present evidence based on R32 expression for a previously unappreciated class of pacemakers that we have called lateral posterior neurons (LPNs), based on their earlier description as Timeless (TIM)-expressing, nonpacemakers by Kaneko and Hall (2000). We define developmental, cellular, and anatomical criteria by which identified neuronal subclasses can be recognized within the LN_d, DN1, DN2, and DN3 classes. Finally, we identify a second candidate neuropeptide transmitter within the *Drosophila* pacemaker network, IPNamide (IPNa), a product of the gene *neuropeptide-like-precursor 1 (nplp1*; Baggerman et al., 2002; Verleyen et al., 2004).

MATERIALS AND METHODS

Fly rearing and strains

Drosophila were reared on cornmeal/agar media supplemented with yeast and kept in either a 25°C incubator or at room temperature. For time-course experiments, flies were entrained to a 12:12 LD cycle for 4–5 days with light intensities of $\sim 3 \times 10^{14}$ W/cm^2 (measured with a LICOR LI250 photo detector) prior to dissection at 25°C. Canton S and y^1w^1 (hereafter referred to as *y w*) flies were used as wildtype controls for colabeling experiments with identical results except for lower background fluorescence in the latter line. The $glass^{60j}$ mutation, used here in a *y w* background, is described by Lindsley and Zimm (1992). Several *cry-gal4* lines were used to drive GFP in clock neurons of interest. They were *cry-gal4[13]* (provided by P. Emery), *cry-gal4[16]* (provided by R. Allada), and *cry-gal4[39]* (provided by F. Rouyer). All three have been shown to drive expression in the LN_vs, LN_ds, in a subset of DNs, and in other nonclock neurons (Zhao et al., 2003; Klarsfeld et al., 2004; Stoleru et al., 2004). We employed *uas-cd8GFP* (Flybase #5137) and *uas-2XeGFP* (Flybase #6874) to visualize neuronal projections. The stable reporter line *y w;tim-gal4(27-1-1), uas-GFP(1010T2)/Cyo*, used here to visualize the DN3s, has been reported previously (Kaneko and Hall, 2000; Helfrich-Förster, 2003).

Isolation of the enhancer trap line R32

The P element insertion line *P{wF6-84 – R32}* is described in this report. It is a single P insertion line generated by mobilization of the *P{wF6-84}* element that is inserted at cytogenic position ~86A5. *P{wF6-84}* is a *P{lacW}* element that drives *lacZ* under the control of a fragment of the promoter for the neuropeptide gene *dFMRFa* (Schneider et al., 1993). *P{wF6-84}* produced ectopic (i.e., non-*dFMRFa*) LacZ labeling that resembled clock neuronal populations, and also harbored a mutation of the *pdf* neuropeptide gene (Renn et al., 1999). It was therefore subjected to mobilization to generate the insertion (and the same ectopic labeling pattern) in a pdf^+ background. Derivative lines of *P{wF6-84}* were either recovered as w^+ (therefore named R lines) or w^- (therefore named W lines); the original P insertion locus and the *pdf* locus were then each analyzed molecularly in derivative lines. The R32 derivative line retains the original 86A *P{lacW}* insertion without damage to the neighboring sequences and contains a wildtype *pdf* genomic sequence. The *P{wF6-84}* insertion site is located less than 100 bp upstream of the transcription start site for the bHLH gene *stich1 (CG17100* – NM080036), which is a site shared by several other recorded P elements—e.g., *P{EP(3)3470}* – AQ074026.

Immunocytochemistry

Adult flies were immobilized with CO_2 and pinned down under Ca^{2+}-free fly saline (pH 7.2) in a dissecting dish by a single insect pin through the thorax. The head cuticle was disrupted using two fine forceps to allow access to the underlying brain. Fifteen to 20 flies were dissected for each timepoint or treatment on a given day and immediately placed in a well of a four-well culture plate containing 4% formaldehyde in phosphate-buffered saline (PBS, pH 7.4) with or without 7% picric acid (the latter was used when colabeling for the neuropeptides PDF and IPNa). Fixation proceeded for 1 hour at room temperature (RT) with gentle agitation, followed by a rinse in PBS. Brains were then isolated by further dissection. Brains were transferred to 2-ml round-bottomed Eppendorf tubes full of PBS-TX (PBS with 0.3% Triton X-100, pH 7.4; Sigma, St. Louis MO) and kept on ice until blocked.

Brains were blocked in 3% normal goat serum in PBS-TX for 45 minutes to 2 hours at RT with gentle agitation, rinsed in PBS-TX, and placed in primary sera for 2 nights at 4°C with gentle agitation. Brains were rinsed with five changes of PBS-TX at RT on a Lab-Quake rotator (Barnstead/Thermoline) for 15 minutes to 1 hour per rinse. Brains were placed in secondary antiserum for 1 night at 4°C with gentle agitation and rinsed as before. Care was taken to treat brains for time-course experiments identically throughout labeling and rinsing. Brains were rinsed in three changes of PBS and mounted in rows on a poly-L-lysine-coated cover slip. Typically, 8–15 brains were mounted for each treatment. Brains were dehydrated in a graded glycerol series (30%, 50%, and 70% in PBS for 5 minutes each). The coverslip was lowered onto a large drop of "Hard-Set" Vectashield fluorescent mounting medium (Vector Laboratories, Burlingame, CA) flanked by two spacer coverslips onto a microscope slide.

The primary antisera used here have all been described previously. All primary and secondary antisera were diluted in PBS-TX. Mouse anti-β-galactosidase (Promega, Madison, WI, Cat. #Z3781, Lot #149211), raised against amino acids 650–926 of *E. coli* β-galactosidase and tested for specificity on dot-blots by the manufacturer, was diluted 1:1,000. Rat anti-PER (provided by M. Rosbash) was raised against a fusion of the first 14 amino acids of the T7 phage coat protein and the C-terminal 1,108 amino acids of PER (Liu et al., 1992). This serum recognizes PER specifically on Western blots and fails to label tissue in per^{01} mutants (Liu et al., 1992). Anti-PER was used at 1:500. The rat anti-TIM serum used here (UPR41, provided by A. Seghal) was raised against His-tagged, full-length TIM and specifically recognizes a TIM band on Western blots that is missing in *tim* null mutants (Amita Sehgal, pers. commun.). Anti-TIM was diluted 1:500. The rabbit anti-PDP1 used here (provided by J. Blau) was raised against a GST-PDP1alpha fusion protein; it recognizes a specific PDP1 band on Western blots, and fails to label tissue in $PDP1^{P205}$ mutant pupae (Cryan et al., 2003). Anti-PDP1 was diluted 1:1,000. Guinea pig anti-proPDF (PAP-59-IV) was raised against amino acids 65–79 of pre-proPDF (H-YPLILENSLGPSVPI-OH) conju-

gated to bovine serum albumin (BSA). This serum fails to visualize the LN_vs in pdf^{01} mutants (Renn et al., 1999). Anti-PDF was used at 1:1,000. Mouse anti-ELAV (mAb Elav-9F8A9 supernatant, Developmental Studies Hybridoma Bank, Iowa City, IA) was raised against a fusion protein consisting of the first 260 amino acids of phage T7 gene and full-length ELAV protein (O'Neill et al., 1994). This anti-ELAV serum detects ELAV-specific bands on Western blots (e.g., Samson et al., 1995) and was used in this study at 1:10. Anti-GLASS (mAb 9B2.1 supernatant, Developmental Studies Hybridoma Bank) was raised against a GLASS-trp E fusion protein, and Glass immunosignals were lost in the photoreceptors of $glass^{60j}$ mutants (Moses and Rubin, 1991). Anti-GLASS was diluted 1:15. Rabbit anti-IPNa (Verleyen et al., 2004) was diluted 1:1,000. The IPNa serum used here was described by Verleyen et al. (2004), and was raised in rabbit against synthetic IPNa peptide (NVGTLARDFQLPIPNamide) coupled to thyroglobulin. Its specificity was determined by solid phase dot blot assays (Verleyen et al., 2004). AlexaFluor 488 and 568-conjugated secondary antisera (all raised in goat; Molecular Probes, Eugene, OR) were used at 1:1,000.

Confocal microscopy

Confocal stacks were obtained by an Olympus Fluoview 500A microscope and Fluoview acquisition software using a 60X/1.20NA water objective lens. Distances were approximated by digital scale bars in Fluoview or by counting the number of 0.5-μm Z-steps between objects in different focal planes. For double-labeling experiments we used only sequential scans of the argon and krypton lasers to avoid bleed-through between channels. When imaging time-course experiments, Fluoview's "Hi-Lo" look-up table was used to set PMT voltage (typically 800 V) and laser power (0.1–4.0%) to minimize peak and trough pixel intensities (i.e., to avoid clipping) in ZT00 preparations (i.e., the most intensely labeled timepoint). Gain was maintained at 1× and offset at 0%. Typically, 5–7 scans were Kalman-averaged for each optical section. These settings were kept constant for all the timepoints of a given experiment and all brains of a given time-course were imaged in the same session with the same brain orientation so that micrographs could be directly compared for labeling intensity. The constituent optical sections of a Z-series were saved as 16-bit multi-TIFF files and exported to Image J for postacquisition analysis and Z-stack construction. Z-stack projections were adjusted for levels and contrast in Adobe Photoshop (San Jose, CA). Micrographs of PER and TIM time-course data were not adjusted in this way. For somatic size comparisons all $DN1_p$ (see below) and LN_d soma of a single hemisphere were imaged by Z-series in five brains per treatment and subsequently digitally isolated from neighboring cells in Photoshop from micrographs of single optical sections.

Observation numbers and presentation of representative micrographs

Unless stated otherwise in the Results, all labeling patterns described here were unanimous within groups of 8–15 mounted brains. Many subsequent replications of each labeling experiment were then undertaken for the purpose of imaging preps in multiple orientations to attain micrographs that revealed well-separated clock neuron groups when presented in a projected Z-series. For PER and TIM time-course analysis, five brains each were imaged for each timepoint and all cell bodies of a given class within a single hemisphere were imaged per brain. The distributions of PER and TIM in these neurons were uniform among brains of a given timepoint and the micrographs presented here were selected on the basis of clarity.

RESULTS

R32-mediated LacZ expression is a highly limited and precise reporter of neuronal PER expression

Immunocytochemical visualization of R32-mediated LacZ expression in the adult brain revealed a pattern that was strikingly similar to that of PER-expressing circadian pacemaker neurons (Fig. 1; cf. Helfrich-Förster, 2003). Clusters of cells resembling all six classes of clock neurons were clearly visible (Fig. 1). In general there was little suggestion of R32-LacZ among populations of smaller (putatively glial) cells. Three groups of R32-positive cells did not correspond to known clock-neuron classes: 1) A cluster of three to four cells in the lateral central brain were medial to the LN_ds and near the posterior surface of the brain (Fig. 1A). We referred to these as lateral posterior neurons (LPNs) pending confirmation as neurons (see below). 2) A single large cell was visible in the medial central brain (Fig. 1A), which we called a large medial cell (l-MC). 3) R32 brains imaged through the dorsal surface revealed two conspicuous cells separated anteriorly from the DN1s by 15–30 μm (Fig. 1B). These cells, which we called anterior DN1s ($DN1_a$s) pending the determination of their neuronal nature (see below), were not clearly distinguished in brains imaged through the anterior or posterior surfaces of the brain because they clustered with the majority of DN1s when all Z-planes were collapsed to a single micrograph as in Figure 1A (see below). To our knowledge the l-MCs and $DN1_a$s are located in brain regions not previously associated with known clock neuron classes (Kaneko and Hall, 2000; Helfrich-Förster, 2003). The LPNs were reminiscent of a cluster of TIM-expressing neurons described by Kaneko and Hall (2000) that were thought not to express PER.

Double labeling of R32 brains dissected at ZT23 in a 12:12 LD cycle (where ZT00 = lights-on) for LacZ and PER revealed that all R32-positive cells except the l-MCs expressed PER at this timepoint (Fig. 2), confirming the clock-neuron-like nature of nearly all R32 labeling. Thus, the LPNs and the $DN1_a$s were considered candidates as previously uncharacterized clock neurons. Such double labeling at ZTs 00, 06, 12, and 18 (i.e., throughout the diurnal cycle) revealed no PER labeling in the l-MCs (data not shown). The l-MCs were not considered further as clock-neuron candidates.

New class of clock neuron: the lateral posterior neurons

R32 brains double-labeled for LacZ and PER or TIM at ZTs 00, 06, 12, and 18 revealed a canonical PER/TIM oscillation in the LPNs under a 12:12 LD cycle: protein levels were high and nuclear at the end of the night and low at the end of the day (Fig. 3A). As visualized by R32, the LPNs always numbered three or four cells. These were consistently situated near the posterior surface of the

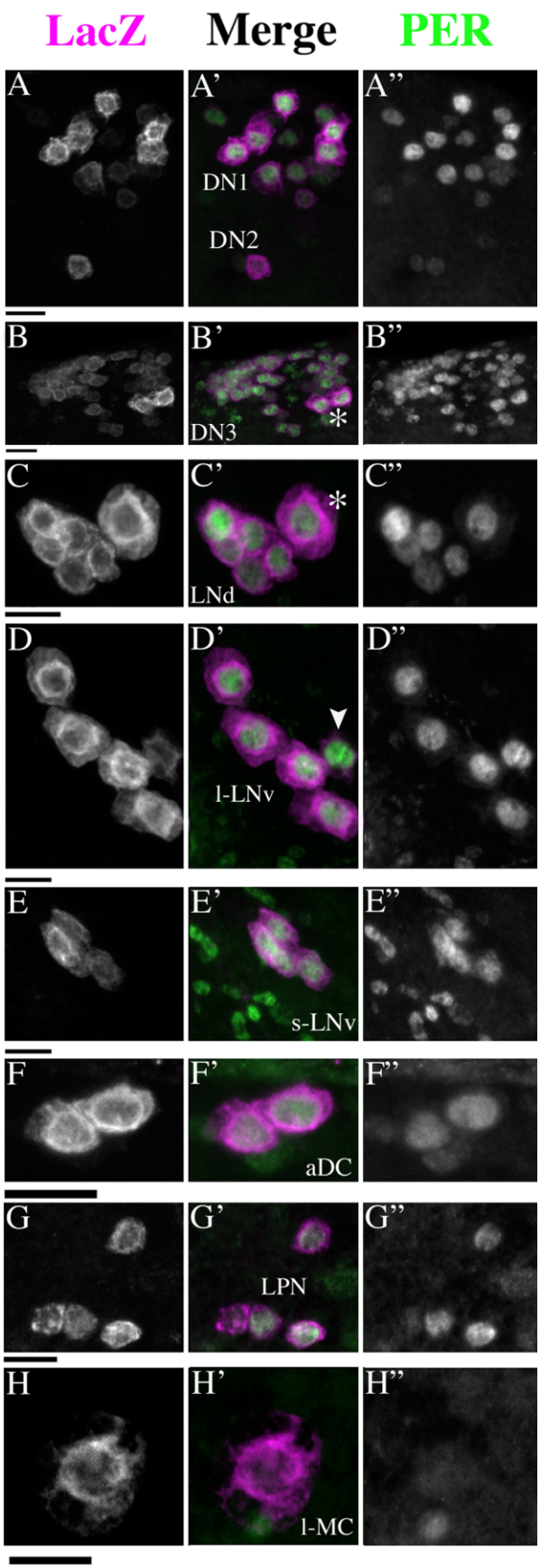

brain and were frequently difficult to visualize beneath the often-high fluorescence of the brain surface. The LPNs resided in anterior/posterior planes near the posterior-most segment of the dorsal PDF projection emanating from the small LN_vs (Fig. 3B–B″). These cells often straddled this projection, but were just as frequently found in positions lateral or medial to it.

To ensure that the presence of the LPNs was not an anomalous aspect specific to the R32 stock, we labeled wildtype brains (from *y w* and CS flies) for PER and imaged brains through the posterior surface. LPNs were clearly visible in all brains as brightly labeled nuclei at ZT23 (Fig. 3C). These nuclei were larger and much brighter than the surrounding small, weakly labeled PER cells. The latter are thought to be glia and compose the largest group of PER-expressing cells in the adult brain (Ewer et al., 1992). To determine the nature of LPNs we colabeled wildtype brains dissected at ZT23 with antisera against PER and ELAV. Every brain revealed a nuclear colocalization of PER and ELAV in all LPNs (Fig. 3D–D″). These results indicate that the LPNs comprise a previously unappreciated class of clock neurons.

DN1 class is divisible into highly reproducible anterior and posterior subclasses.

R32 brains double-labeled for LacZ and PER or TIM at ZTs 00, 06, 12, and 18 revealed a canonical PER/TIM oscillation in the $DN1_a$s under a 12:12 LD cycle (Fig. 4A). As described above, the $DN1_a$s were separated anteriorly from the DN1s by 15–30 μm in R32 brains. We sought to describe the location of these cells in more detail. R32 brains were double-labeled for LacZ and PDF, the latter as an anatomical reference. The relative positions of the DN2s, DN1s, and the $DN1_a$s are most easily observed in brains imaged through the posterior aspect of the brain, but with a slight anterior bias (i.e., the brains were mounted with the posterior surface mounted against the coverslip with a slight tilt toward the dorsal surface). In brains so mounted the DN2s were always closely associated with the dorsal PDF projection, often within or ventral to the expanse of its termini, the DN1 were situated just above (i.e., dorsal) to the PDF projection, and the $DN1_a$s were further removed from the PDF projection and often closer to the dorsal brain surface than either class of DN (Fig. 4B).

Using 0.5-μm Z-steps, brains mounted without an anterior bias were imaged through the posterior surface where imaged to a depth of 100 μm as a means of visualizing the relative positions of the $DN1_a$s and DN1s in the anterior/posterior axis. The $DN1_a$s were always separated by at least 15 and up to 30 μm anteriorly from the DN1s.

Fig. 2. PER expression in R32-positive cells. R32 LacZ labeling is shown in the left column (**A–H**). The center column presents merged micrographs with R32-LacZ in magenta and PER in green (A′-H′). PER labeling is shown in the right column (A″-H″). A: The DN1 and DN2. B: The DN3, the asterisk in B′ indicates two large cells. C: Six LN_d, asterisk in C′ indicates a single large cell. D: Four large LN_v and fifth small LN_v (indicated by the arrowhead in D′). E: Four small LN_v, the smaller PER-positive cells are presumably glia. F: Two $DN1_a$s. G: Four LPNs, one cell is expressing PER very weakly. H: A single l-MC, no clear PER immunoreactivity was detected in these cells. Scale bars = 10 μm.

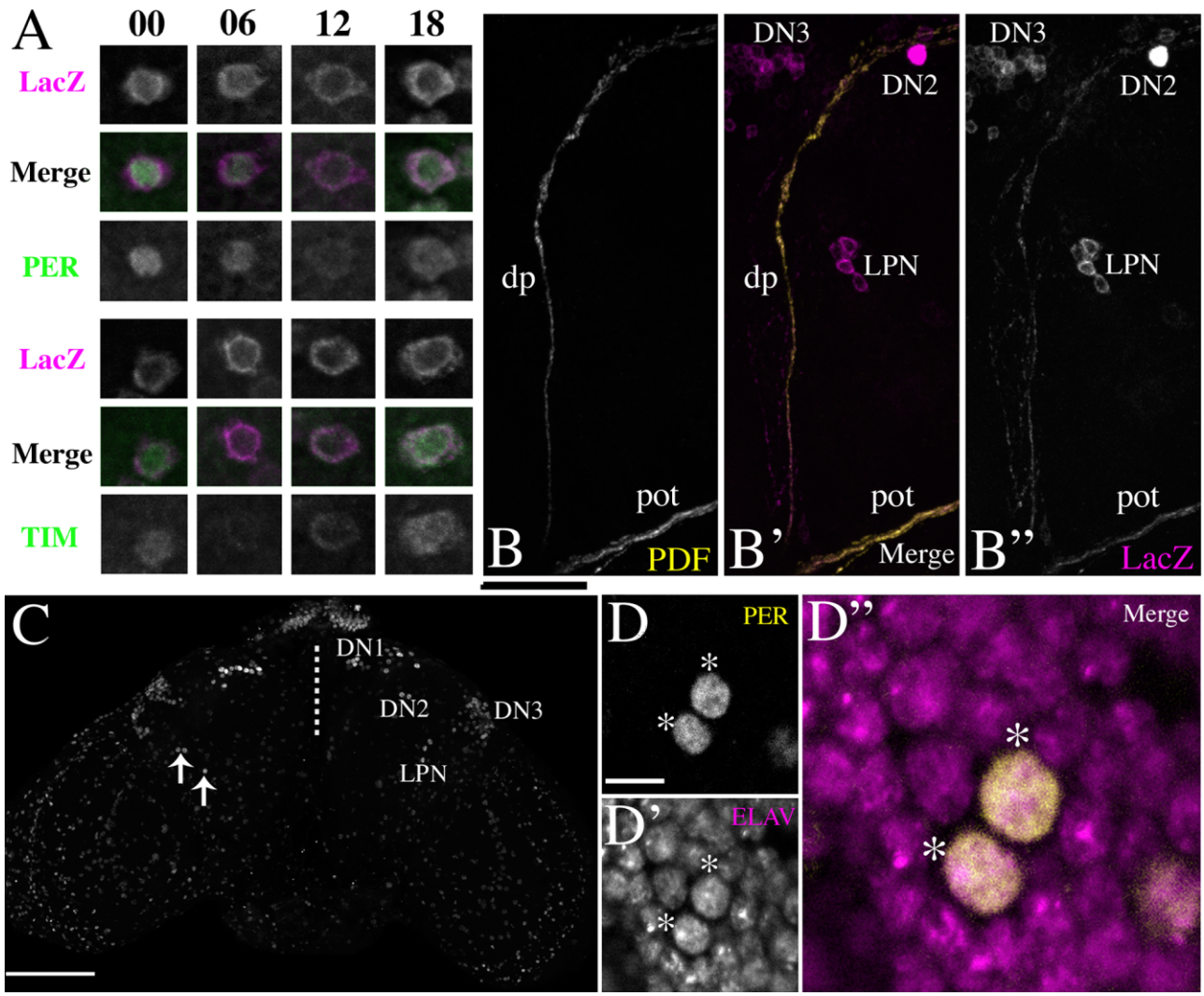

Fig. 3. The LPNs express PER and TIM with a diurnal rhythm, are consistently situated near the posteriormost segment of the dorsal PDF projection, are present in wildtype brains, and express the neuronal marker ELAV. **A:** Representative micrographs of LPNs colabeled for R32 LacZ and PER (top panel) or R32 LacZ and TIM (bottom panel) at various times of day in a 12:12 LD cycle. Numbers indicate Zeitgeber Times. Merged micrographs are presented with R32 LacZ in magenta and PER and TIM in green. **B:** A Z-series with a depth of 5 μm through a portion of the dorsal PDF projection. B′: Merged Z-series of PDF projection (yellow) and R32lacZ (magenta). B″: Single-labeled Z-series of R32-Laz containing the LPN. The brain was imaged through the posterior surface of the brain. pot, posterior optic tract; dp, dorsal projection. **C:** A partial Z-series through the posterior half of a *y w* brain dissected at ZT23 and labeled for PER protein. Arrows in the left hemisphere indicate LPNs. The dashed line represents the midline. **D:** A single optical section through two LPNs labeled for PER at ZT 23. D′: The same optical section labeled for ELAV. D″: A merged micrograph with PER in yellow and ELAV in magenta. In D–D″ the colabeled neurons are marked by asterisks. Scale bars = 20 μm in B; 100 μm in C; 5 μm in D. [Color figure can be viewed in the online issue, which is available at www.interscience.wiley.com.]

Thus, $DN1_a$s were situated further away from the DN1s than were the DN2s. However, this was only apparent when the dorsal cells were imaged from the dorsal aspect of the brain or when relative Z-depths were accounted for in brains mounted in the anterior or posterior aspect. Clock neurons have traditionally been imaged in the anterior or posterior aspect. When imaged this way the $DN1_a$s of R32 brains usually appeared clustered with the DN1s. Therefore, when the Z-planes were collapsed the $DN1_a$s were not discernable from the DN1s (cf. Fig. 1A,B). We therefore wondered if the $DN1_a$s were truly not-previously-described clock cells or if they had been grouped with DN1s without reference to their anterior isolation (see below).

The $DN1_a$s were clearly visible in wildtype brains as brightly labeled nuclei at ZT23 in brains imaged through the dorsal surface (Fig. 4C). Thus, the presence of $DN1_a$s was not an anomalous aspect specific to the R32 stock. To determine the nature of $DN1_a$s we colabeled wildtype brains dissected at ZT23 with antisera against PER and ELAV. Every brain revealed a nuclear colocalization of PER and ELAV in all $DN1_a$s (data not shown). We hereafter refer to the larger and more posterior group of DN1s as posterior DN1s ($DN1_p$).

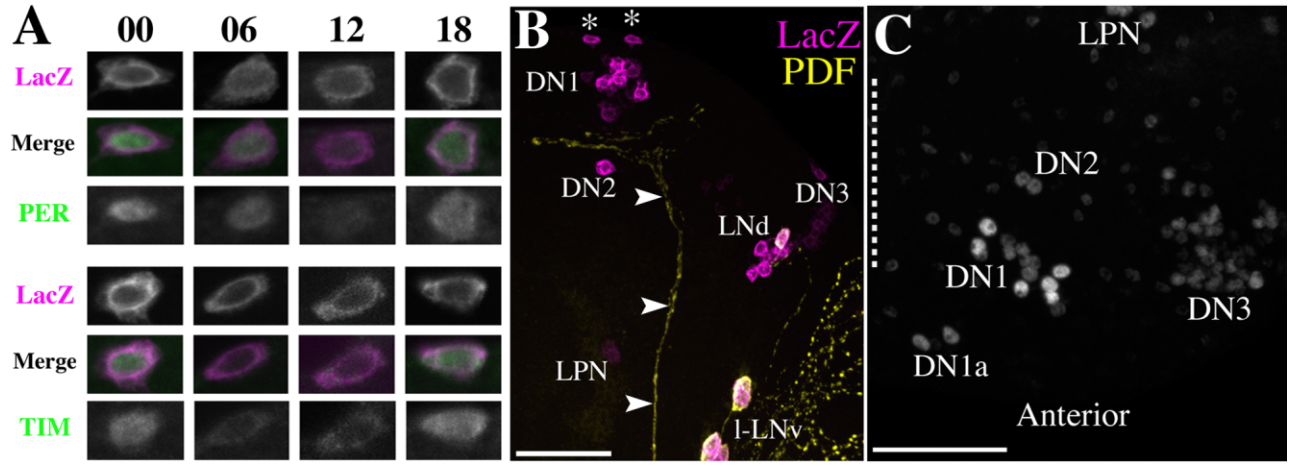

Fig. 4. The $DN1_a$s express PER and TIM with a diurnal rhythm and are consistently situated in dorsal brain regions anterior to the DN2, DN1s, and PDF terminals. **A:** Representative micrographs of $DN1_a$s colabeled for R32 LacZ and PER and R32 LacZ and TIM at various times of day in a 12:12 LD cycle. Numbers indicate Zeitgeber Times. Merged micrographs are presented with R32 LacZ in magenta and PER and TIM in green. **B:** A Z-series with a depth of 52 μm through the dorsoposterior surface (see text) of an R32 brain colabeled for R32 LacZ (magenta) and PDF (yellow). The $DN1_a$s are indicated by asterisks and lie just beneath the dorsal surface of the brain. The dorsal PDF projection is indicated by arrowheads. **C:** A Z-series with a depth of 26 μm through the dorsal surface of a *y w* brain dissected at ZT23 and labeled for PER. The dashed line indicates the midline. The $DN1_a$s are visible as two PER-positive nuclei anterior and medial to the DN1s. Scale bars = 50 μm in B; 50 μm in C. [Color figure can be viewed in the online issue, which is available at www.interscience.wiley.com.]

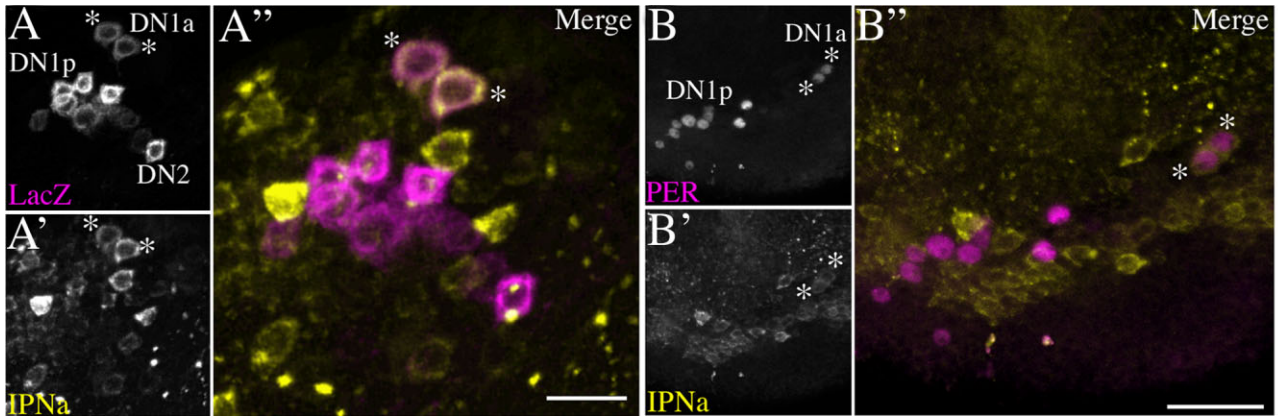

Fig. 5. The $DN1_a$ express the neuropeptide IPNa. **A:** A Z-series with a depth of 75 μm through posterior surface of an R32 brain labeled for R32 LacZ. A′: The same Z-series for IPNa labeling. A″: A merged micrograph of IPNa (yellow) and R32-LacZ (magenta). Dorsal is up. Asterisks indicate IPNa expression in the $DN1_a$ in A–A″. **B:** A Z-series with a depth of 17 μm through the dorsal surface of a *y w* brain dissected at ZT23 and labeled for PER. B′: The same Z-stack for IPNa labeling. B″: The merged micrographs with PER in magenta and IPNa in yellow. Anterior is up. Asterisks indicate IPNa expression in the $DN1_a$. Scale bars = 10 μm in A; 20 μm in B. [Color figure can be viewed in the online issue, which is available at www.interscience.wiley.com.]

$DN1_a$ are labeled by antibodies of an *nplp1*-derived neuropeptide

The neuropeptide IPNamide (IPNa) is widely expressed throughout the brain and ventral nerve chord of the fly (Verleyen et al., 2004). During an immunocytochemical screen of neuropeptides for expression in clock-neurons we found that antibodies directed against IPNa peptide derived from the NPLP1 precursor (Verleyen et al., 2004) specifically label the $DN1_a$ cell bodies. R32 brains double-labeled for LacZ and IPNa showed clear colocalization in the $DN1_a$ but not the $DN1_p$ and DN2s (Fig. 5A–A″). Likewise, wildtype brains dissected at ZT23 revealed cytoplasmic IPNa labeling around the PER-positive $DN1_a$ nuclei (Fig. 5B–B″). Thus, in addition to their anatomical isolation, the $DN1_a$ were differentiated from the $DN1_p$ by virtue of their IPNa expression. The $DN1_a$ represented a small minority of total IPNa labeling in the adult brain (cf. Verleyen et al., 2004) and this neuropeptide was expressed by soma that were distinct from but quite close to the $DN1_p$ (Figs. 5, 6).

$DN1_a$ are developmentally distinct from the $DN1_p$

The *glass* mutation, which causes the loss of all external photoreceptors, was determined by Helfrich-Förster et al.

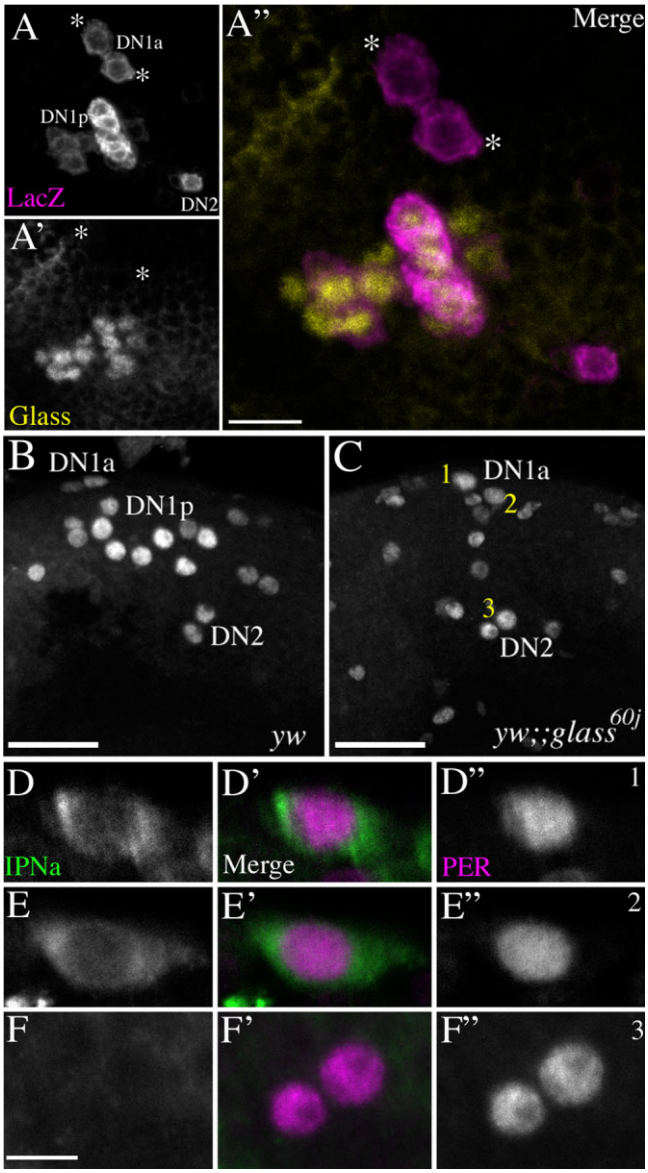

Fig. 6. The $DN1_a$ do not express GLASS and survive the *glass* mutation. **A:** A Z-series with a depth of 23 μm through the $DN1_a$, $DN1_p$, and DN2 in an R32 brain, labeled for LacZ. A′: the same Z-series for GLASS labeling. A″: A merged micrograph of LacZ (magenta) and IPNa (yellow) labeling. Only the $DN1_p$ expressed glass. In A–A″ the positions of the $DN1_a$ are indicated by asterisks. This preparation was imaged through the posterior surface of the brain. Dorsal is up. **B:** PER expression in a *y w* brain dissected at ZT23. **C:** PER expression in a *y w;;glass*^{60j} brain dissected at ZT23. Z-series in C and **D** are 80 μm deep and both brains were imaged through the posterior surface. Dorsal is up. Laser power was higher for the *y w;;glass*^{60j} micrograph (C) to ensure the detection of all weakly PER-positive cells. For this reason PER-positive glia are visible in B but not in C. The numbering of the DN1s as 1 and 2 and the DN2 as 3 in C are for reference in the following panels. D–D″: A single optical section of the DN1 labeled 1 in panel C labeled for IPNa (D) and PER (D″) the merged image is shown in D′ with IPNa in green and PER in magenta. **E–E″:** A single optical section of the DN1 labeled 2 in panel C labeled for IPNa (E) and PER (E″) the merged image is shown in E′ with IPNa in green and PER in magenta. **F–F″:** A single optical section of the DN2s labeled 3 in C, labeled for IPNa (F) and PER (F″). The merged image is shown in F′ with IPNa in green and PER in magenta. The surviving DN1 (neurons 1 and 2 in C) display cytoplasmic IPNa (D and E), while the DN2s (labeled 3 in C) do not express this peptide (F). Scale bars = 10 μm in A; 20 μm in B,C; 5 μm in D. [Color figure can be viewed in the online issue, which is available at www.interscience.wiley.com.]

(2001) to result in the loss of all but two DN1s. We wondered if the *glass*-surviving DN1s were the two $DN1_a$. Klarsfeld et al. (2004) established that all but two DN1s express GLASS, a transcription factor necessary for photoreceptor differentiation (Moses et al., 1989). Therefore, we first asked if the $DN1_a$ express GLASS protein. R32 brains were double-labeled for LacZ and GLASS and imaged through the posterior aspect of the brain. $DN1_a$ were identified by virtue of their anterior location relative to the $DN1_p$. In all brains the $DN1_p$ expressed GLASS and the $DN1_a$ did not (Fig. 6A–A″: cf. Klarsfeld et al., 2004). We therefore predicted that the two glass-surviving DN1s would be the $DN1_a$. To test this supposition, *y w* and *yw;;glass*^{60j} brains were dissected at ZT23 and colabeled for PER and IPNa, the latter as a marker for the $DN1_a$. These brains were imaged through the posterior surface of the dorsal brain by a Z-series that commenced a few microns posterior from (i.e., superficial to) the DN2 to a depth of 80 μm, such that a Z-series always included all DN1s and DN2s of wildtype flies with tens of microns to spare. As expected, *y w* brains showed the normal contingent of 14–17 DN1 (Fig. 6B; Kaneko and Hall, 2000; Helfrich-Förster, 2003), while the *y w;;glass* brains showed only two DN1 (Fig. 6C; Helfrich-Förster et al., 2001). Single optical sections through the surviving DN1 of *glass* mutants revealed their expression of IPNa (Fig. 6D–E″). Identical scans through the DN2 neurons in *glass* mutants revealed no such expression (Fig. 6F–F″). We conclude that *glass* mutants lack all $DN1_p$s and retain the $DN1_a$s.

The larval brain contains fewer clock-expressing neurons than the adult: just four to five LN_vs, two DN2s, and two DN1s (Kaneko and Hall. 2000). Klarsfeld et al. (2004) hypothesized that the two DN1s that lacked GLASS expression in the adult were the same DN1s present in larvae. We therefore predicted that the larval DN1s would express IPNa. We initially conducted colabeling experiments in R32 larvae, but LacZ labeling revealed many nonclock neurons (Fig. 7A–A″), making it difficult to identify the larval DN1s unambiguously. We therefore conducted larval labeling in brains doubly heterozygous for *Cry-gal4[16]* and *uas-cd8GFP*. Only the LN_vs and DN1s are clearly marked in such brains (Fig. 7B; Klarsfeld et al., 2004). IPNa was always detectable in the larval DN1 (Fig. 7B–B″). As predicted by Klarsfeld et al. (2004), these results support the hypothesis that the $DN1_a$ in the adult nervous system represent persistent larval DN1s.

$DN1_a$ project toward the PDF terminals and accessory medulla

Kaneko and Hall (2000) observed that the DN1s were not homogeneous in their axonal projections. Whereas most DN1s sent projections either medially or laterally across the superior protocerebrum, a smaller number of DN1s traced the dorsal PDF projection of the s-LN_vs down toward the accessory medulla, while a few others projected ventrally toward the midline along the posterior surface of the brain toward the esophageal foramen (Kaneko and Hall, 2000). We wondered which of these projection patterns the $DN1_a$ followed. We visualized the projections of the larval DN1s and the adult $DN1_a$ through the directed expression of GFP or cd8GFP, driven by one of several *Cry-Gal4* elements (see Materials and Methods). Larval DN1s project directly toward the PDF terminals of the LN_vs (Kaneko and Hall, 2000; Fig. 8A) and

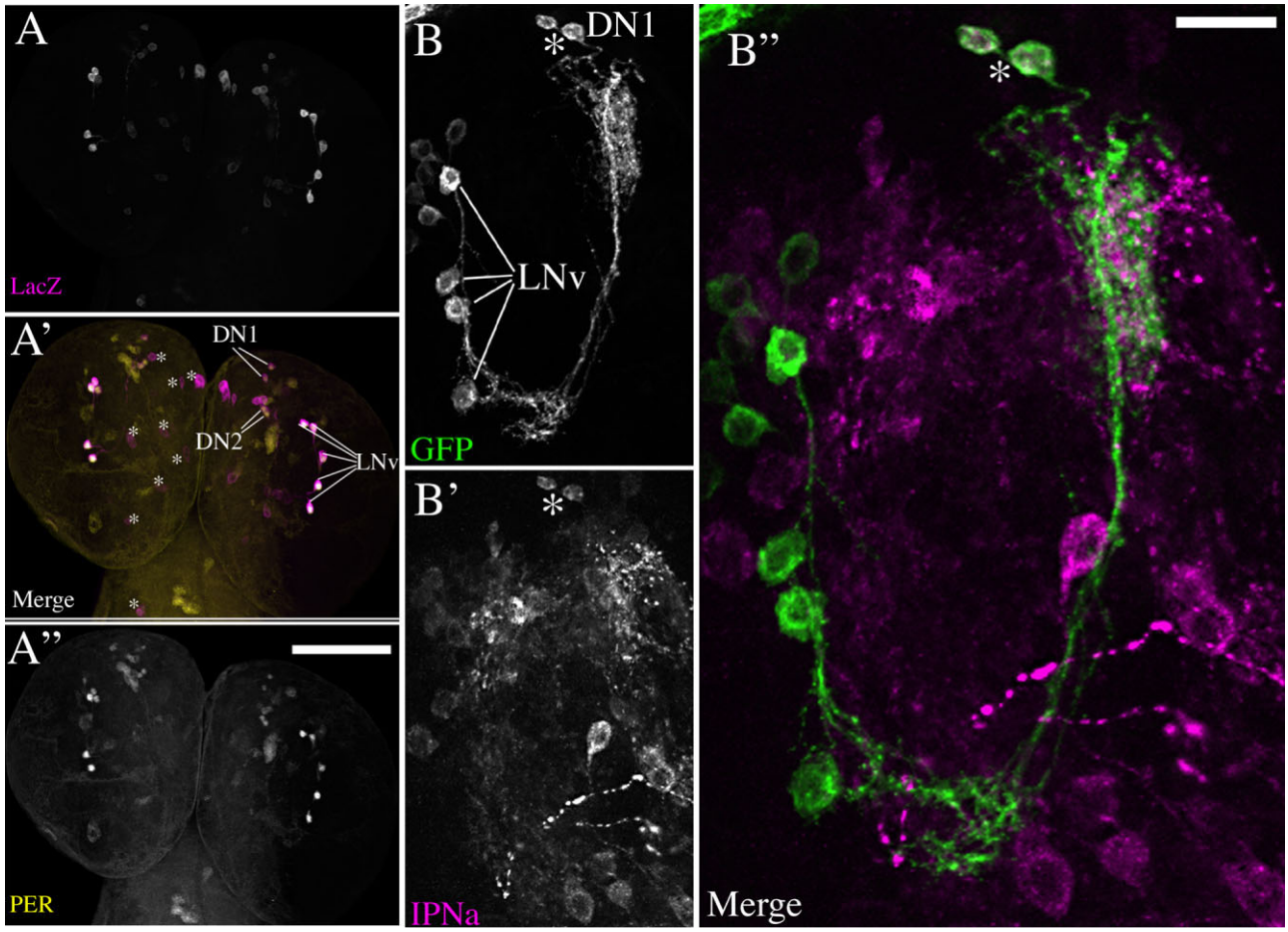

Fig. 7. The larval DN1s express IPNa. **A:** A Z-series with a depth of 31 μm from an R32 larval brain labeled for LacZ at ZT 23. A′: A merged micrograph of the same Z-series for LacZ (magenta) and PER (yellow). A″: The same Z-series for PER only. LacZ expression in the larval brain reveals many neurons that do not express PER. These are marked with asterisks in the left hemisphere in A′. **B:** A Z-series with a depth of 22 μm within a larval brain containing the targeted expression of GFP by *Cry-gal4(16)*. Visualization of GFP reveals the larval DN1s and LN_vs, but not the DN2s. B′: IPNa labeling in the same Z-series. B″: Merged micrographs of IPNa (magenta) and GFP (green). IPNa was expressed in both larval DN1s. An asterisk indicates the position of the DN1s in B–B″. Scale bars = 20 μm. [Color figure can be viewed in the online issue, which is available at www.interscience.wiley.com.]

form an adjacent net of termini (Fig. 8B). It is possible that the larval DN1 projection continues down the length of the PDF projection (Kaneko and Hall, 2000), but the preparations reported here did not allow for the unambiguous tracking of larval DN1 projections past the PDF termini. In the dorsal brain of *Cry-Gal4[13]/uas-GFP* adults, the $DN1_a$ were clearly visible, as were two $DN1_p$ and two DN3 (Fig. 8C), *Cry-Gal4[13]* also drove GFP in all s-LN_v, l-LN_v, and LN_d (Klarsfeld et al., 2004; Stoleru et al., 2005; Fig. 8C). In all brains observed the $DN1_a$ projected toward the dorsal PDF termini. In most cases the $DN1_a$ projections joined this bundle of neurites and were impossible to track with confidence. Nevertheless, in several preparations at least one of the $DN1_a$ projections flanked this bundle of neurites without joining it (Fig. 8C,D). In such cases the $DN1_a$ projected ventrally toward the accessory medulla (Fig. 8C,D). We conclude that the $DN1_a$ projections maintain their association with the dorsal PDF projection after metamorphosis and that the $DN1_a$ are at least partly responsible for the innervation of the accessory medulla by the DN1 pacemaker neuron class.

R32 reveals diversity within clock-neuron classes

High-magnification imaging of R32 soma revealed unexpected diversity within previously characterized clock-neuron classes. For example, we found that the $DN1_p$s were heterogeneous with respect to soma size and labeling intensity. Approximately half of the 14–17 $DN1_p$ somata were larger and displayed more intense R32-LacZ and PER labeling at ZT23 (Fig. 2A–A″). The DN2 pacemaker class was also reproducibly divisible by R32-LacZ labeling intensity (Fig. 2A). In most brains the more weakly labeled DN2 soma was clearly present, as visualized by PER labeling (Fig. 2A–A″). In R32 brains two large and intensely labeled DN3s stood in contrast to their typically small and weakly labeled neuronal congeners (Fig. 2B). The LN_ds also showed one to three cells that were clearly larger than the others (Fig. 2C). Although these results

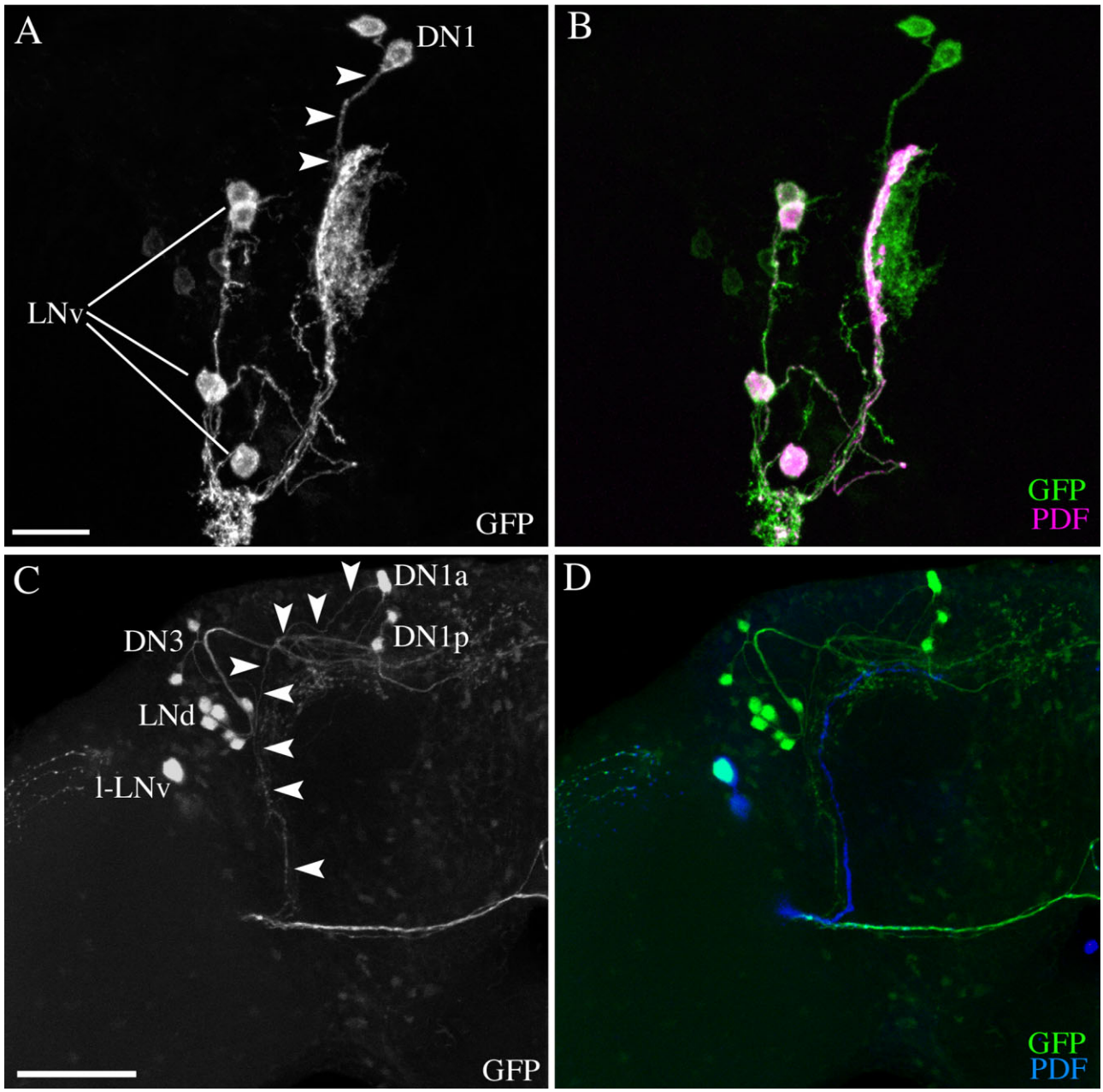

Fig. 8. The projections of larval DN1s and adult $DN1_a$s are closely associated with the dorsal PDF projection. **A,B:** A Z-series with a depth of 44 μm through the DN1 and LN_v of a *Cry-Gal4(16)/uas-cd8GFP* larval brain labeled for PDF. A: GFP only. Arrowheads mark the projection of the DN1s. B: A merged micrograph of GFP (green) and PDF (magenta). Note the GFP-only terminals to the right of the PDF projection. These presumably arise from the DN1s. **C:** A Z-series through the DNs and LN_ds of a *Cry-gal4(13)/uas-GFP*, displaying GFP only. The $DN1_a$s are visible in this series as are two $DN1_p$, two DN3, six LN_ds, and one l-LN_v. The projection of a single $DN1_a$ is marked with arrowheads. **D:** A merged micrograph of GFP (green) and PDF (blue) from the same Z-series. This represents an atypical preparation in which a $DN1_a$ projection could be discerned from the dorsal PDF projection and followed to the accessory medulla. Scale bars = 20 μm in A (applies to B); 50 μm in C (applies to D).

suggest diversity among the $DN1_p$ and LN_d, quantification and analysis of their areas did not reveal two clear classes of cell bodies, as has been established for the large and small LN_v (data not shown).

We wondered if a similar diversity of soma size was also evident in the LN_d, $DN1_p$, and DN3 of wildtype flies. For the LN_d and $DN1_p$, wildtype (CS) brains were dissected at ZT18 and double-labeled for the clock proteins PER and PDP1. At this time we observed predominantly cytoplasmic PER and nuclear PDP1 (Fig. 9B,D; cf. Cyran et al., 2003). In all brains there was a clear diversity of soma sizes within the LN_d and $DN1_p$ similar to that seen in R32 brains, with cell bodies displaying a smooth range of soma sizes (Fig. 9A–D). Micrographs of individual cell bodies

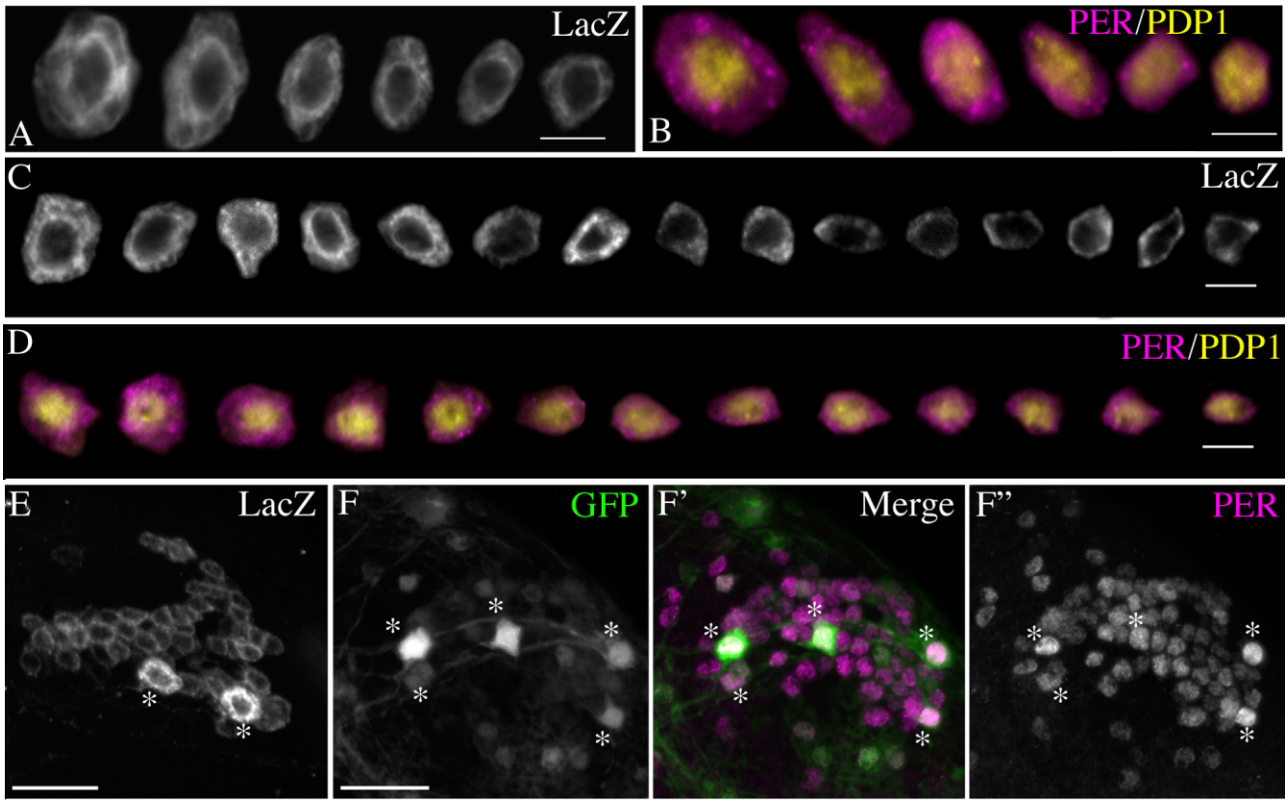

Fig. 9. The LN_d, $DN1_p$, and DN3 each display a variety of soma sizes. **A:** Single optical sections through all LN_ds of a single R32 brain hemisphere labeled for LacZ were visually isolated from neighboring cells and ranked qualitatively from largest to smallest diameter. **B:** A like ordering of all LN_ds from a single hemisphere of a wildtype brain colabeled for PER (magenta) and PDP1 (yellow) at ZT18. **C:** All $DN1_p$s from a single hemisphere of an R32 brain labeled for LacZ and presented as above. **D:** All $DN1_p$s from single hemisphere of a wildtype brain co-labeled for PER (magenta) and PDP1 (yellow) at ZT18. **E:** A 12-μm Z-series through the DN3s from an R32 brain labeled for LacZ. DN3s were imaged through the dorsal surface of the brain. Asterisks indicate two large DN3s. **F:** A 13-μm Z-series through the DN3s in *Tim-Gal4/uas-gfp* brain dissected at ZT23 and visualized for GFP. F′: The same Z-series as a merged micrograph of GFP (green) and PER (magenta) expression. F″: The same Z-series showing PER expression only. DN3s were imaged as in E. Asterisks in F–F″ indicate five larger neurons among the DN3. Scale bars = 5 μm in A–D; Scale bar = 20 μm in E,F. [Color figure can be viewed in the online issue, which is available at www.interscience.wiley.com.]

from the same hemisphere were isolated visually and cell body sizes were ranked qualitatively. This evaluation suggested that, unlike the LN_vs, the LN_d and $DN1_p$ classes could not be divided into unambiguous "large" and "small" cell body groups. Instead, these classes reproducibly displayed smoothly graded cells size differences (Fig. 9A–D). Finally, among the ~40 neurons of the DN3 class, R32 consistently revealed two large and intensely labeled cell bodies (Figs. 2B, 9E). PER/PDP1 labeling in the DN3 was difficult to interpret because the DN3 somata are so densely arranged (data not shown). We therefore labeled brains that were doubly heterozygous for *tim-gal4* and *uas-GFP* elements for PER and imaged the DN3s through the dorsal surface of the brain. In these preparations, four to five cells were clearly larger than the majority of the DN3s and usually expressed higher levels of GFP (Fig. 9F–F″). We propose that, similar to the LN_v classes, the LN_d, $DN1_p$, DN2, and DN3 are not homogenous groups. Rather, each class may well contain identifiable neuronal subsets that will be distinguished in the future by separable molecular and anatomical phenotypes.

DISCUSSION

The recognition of identified classes of neuronal pacemakers offers the possibility of analyzing behaviorally relevant neural circuits in the context of molecularly defined neuronal hierarchies. Ideally, such analysis will account for how individual neuronal pacemakers function and interact to generate and organize rhythmic outputs. To complement and extend previous work in this area, we used imaging techniques to describe the properties of circadian pacemaker neurons in *Drosophila*'s central brain. Here we employed the novel enhancer trap line R32 to reveal several previously undescribed features of the fly's neuronal clockwork (summarized in Fig. 10). In addition to presenting new subclasses of pacemakers, this study reveals a previously uncharacterized diversity within the canonical neuronal pacemaker classes.

Lateral posterior neurons

Kaneko and Hall (2000) identified a group of cells in the posterolateral brain that expressed TIM but not PER, the

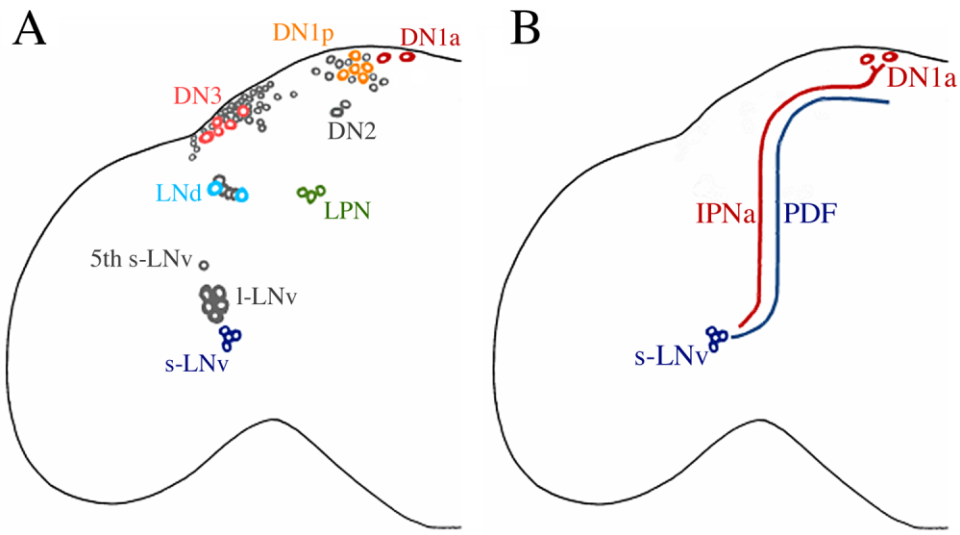

Fig. 10. A reevaluation of the fly's neuronal clockwork. **A:** A map of clock neuron soma in the adult brain of *Drosophila*. The schematic represents only one hemisphere. Our data revealed two new classes of clock neurons, the LPNs and the $DN1_a$s. The canonical DN1s have been redesignated $DN1_p$s. Our results also revealed a diversity of soma sizes within the LN_ds, DN3, and $DN1_p$s. Larger cell bodies are presented in color. **B:** Peptidergic and anatomical interactions between the s-LN_v and the $DN1_a$. Our data revealed that $DN1_p$s express IPNamide. The $DN1_a$s project toward the dorsal PDF projection and in some cases ventrally and anteriorly toward the accessory medulla. [Color figure can be viewed in the online issue, which is available at www.interscience.wiley.com.]

lack of which precluded their identification as neuronal pacemakers. Subsequently, Klarsfeld et al. (2004) alluded to PER-positive cells reminiscent of the TIM-only cells, but could not unambiguously identify them as neurons. Our data revealed a group of cells whose position and number suggest identity with this novel group. We have shown that these cells are indeed neurons (Fig. 3D–D″) and that they are diurnally rhythmic—they express both PER and TIM with a rhythm under LD conditions (Fig. 3A). We have referred to these cells, in deference to Kaneko and Hall (2000), as lateral posterior neurons (LPNs) and their recognition as pacemakers now permits investigation of their specific contributions to circadian physiology. During the preparation of this report, a study by Yoshii et al. (2005) reported that the LPN support a PER oscillation under temperature cycles and constant light, but did not detect such rhythms under LD conditions. These results, along with the detection of PER expression under LD in our study, suggest that the PER/TIM oscillations are stronger under temperature entrainment than under LD conditions, suggesting a special role for these neurons in temperature entrainment (Yoshii et al., 2005).

Anterior DN1s

Klarsfeld et al. (2004) previously described two dorsally separated DN1s and, based on GLASS labeling, hypothesized that these were the persistent larval DN1s. Furthermore, Kaneko and Hall (2000) could often identify the persistent larval DN1s as medially isolated in metamorphosing pupae. In the present study the isolated $DN1_a$ were often but not always found in brain regions medial and dorsal to the rest of the DN1s. Imaging of R32 brains through the dorsal aspect of the brain revealed an even more striking anterior separation of two DN1s that was not previously noted (Figs. 1B, 4B,C). These two neurons are situated further from the majority of DN1s ($DN1_p$s) than were the DN2 (Figs. 1B, 4C). The $DN1_a$s, unlike the $DN1_p$s, expressed the neuropeptide IPNa (Fig. 5), but did not express the transcription factor GLASS (Fig. 6; Klarsfeld et al., 2004). IPNa labeling in larvae suggested that the two larval DN1s persist through metamorphosis as the anteriorly separated $DN1_a$s (Fig. 7B–B″). Thus, we submit that the DN1s as previously classified (reviewed in Helfrich-Förster, 2003) actually comprise at least two distinct classes of clock neurons that are distinguishable by anatomical, immunological, genetic, and developmental criteria. Specifically, the $DN1_a$ are situated in dorsal brain regions 15–30 μm anterior of the $DN1_p$ and DN2s, express the neuropeptide IPNa, do not express GLASS, survive the *glass* mutation, and represent the persistent DN1s of larvae. The $DN1_p$ are located in the posterior region of the dorsal brain adjacent to the dorsal PDF projection, do not express IPNa immunosignals, are unified by GLASS expression, and are missing in adult *glass* mutants. The morphological and phenotypic diversity we ascribe to the two subclasses of DN1 pacemakers suggests a corresponding functional diversity within DN1z. We submit that as our knowledge of clock-cell properties grows such distinctions will permit a fuller accounting for the division of labor between and within the clock neuron classes.

Evidence for peptidergic pacemaker feedback to the accessory medulla

The mammalian suprachiasmatic nucleus, which houses the rhythmic circuits that control circadian locomotor rhythms in mammals, displays multiple transmitter phenotypes (Leak and Moore, 2000). In *Drosophila* multiple amidated peptides are required for normal circadian locomotor rhythms (Taghert et al., 2001), but to date only PDF has been identified as a clock-relevant transmitter (Renn et al., 1999). Here we have shown that the $DN1_a$

pacemakers express IPNa (Figs. 5, 6D–E″), thus implicating *nplp1*-derived peptides as additional candidate clock output factors. We have determined that the $DN1_a$ project axons toward the dorsal PDF projection and then further on to the accessory medulla (Fig. 8). Taken together, these data suggest peptidergic interactions between the accessory medulla and the dorsal brain via PDF and IPNa (Figs. 7B–B″, 8, 10B). Such interactions between clock centers could subserve the synchronization of pacemakers, the maintenance of rhythmicity, or the regulation of its amplitude (cf. Peng et al., 2003; Lin et al., 2004).

Evidence for cellular diversity within clock neuron classes

R32 revealed a replicable diversity of cell body sizes within the $DN1_p$, DN2, DN3, and LN_d classes (Figs. 2, 9). The LN_vs have long been divided into large and small classes and differ in details of their molecular timekeeping (e.g., Yang et al., 2001; Shafer et al., 2002) and their genetic regulation (e.g., Park et al., 2000). Although the LN_ds and the DNs were not neatly divisible into large and small subclasses, the morphological diversity displayed within the DN3s suggests fundamental functional differences similar to those of the LN_v. We submit that the recognition of such phenotypic distinctions will be of great practical importance as attention is turned toward the physiology of individual circadian clock neurons. Fluorescent probes of neuronal excitability are now being employed to study the physiology of single identified neurons in *Drosophila* (e.g., Suh et al., 2004). As such tools are brought to bear on the circadian system, the ability to recognize subclasses of pacemaker neurons will be a necessary adjunct to physiological analysis in situ.

Advantages of R32 as a clock-neuron reporter

Under the conditions reported here, R32-mediated LacZ expression is an exceptionably clear marker of clock neurons. This is due to the strong and widespread expression of LacZ in neuronal pacemakers, the apparent absence of glial labeling, the very low numbers of nonclock-neurons labeled, and the fact that most of the neuronal projections of the clock neurons are invisible or very weakly labeled. Compared to the direct immunocytochemical detection of clock proteins or the use of Gal4-driven GFP (e.g., Kaneko and Hall, 2000), R32 offers a much clearer visualization of clock neurons, even when the entire brain is reconstructed as a projected Z-series (Fig. 1A). These factors, coupled with the relative ease of immunocytochemical detection of LacZ, make R32 an effective clock neuron reporter, particularly for colabeling experiments aimed at determining the neurochemical phenotypes of clock neurons. The regulatory sequences that drive R32-mediated expression have not yet been identified. The possibility that R32 reports on a gene that normally functions within or in proximity to the molecular pacemaker has not yet been explored and cannot be excluded. The utility of the R32 *P{lacW}* insert may be expanded in the future if it proves convertible into a Gal4 and/or Gal80 element, as has been demonstrated for other elements (Sepp and Auld, 1999).

ACKNOWLEDGMENTS

We thank Justin Blau, Michael Rosbash, Liliane Schoofs, and Amita Sehgal for antibodies and Ravi Allada, Patrick Emery, and François Rouyer for fly stocks.

LITERATURE CITED

Baggerman G, Cerstiaens A, De Loof A, Schoofs L. 2002. Peptidomics of the larval *Drosophila melanogaster* central nervous system. J Biol Chem 277:40368–40374.

Cyran SA, Buchsbaum AM, Reddy KL, Lin MC, Glossop MR, Hardin PE, Young MW, Storti RV, Blau J. 2003. *vrille, Pdp1*, and *dClock* form a second feedback loop in the *Drosophila* circadian clock. Cell 112:329–341.

Dunlap JC. 1999. Molecular bases for circadian clocks. Cell 96:271–790.

Ewer J, Frisch B, Hamblen-Coyle MJ, Rosbash M, Hall JC. 1992. Expression of the *period* clock gene within different cell types in the brain of *Drosophila* adults and mosaic analysis of these cells' influence on circadian behavioral rhythms. J Neurosci 12:3321–3349.

Frisch B, Hardin PE, Hamblen-Coyle MJ, Rosbash M, Hall JC. 1994. A promoterless *period* gene mediates behavioral rhythmicity and cyclical *per* expression in a restricted subset of the *Drosophila* nervous system. Neuron 12:555–570.

Grima B, Chélot E, Xia R, Rouyer F. 2004. Morning and evening peaks of activity rely on different clock neurons of the *Drosophila* brain. Nature 431:869–873.

Hall JC. 2005. Systems approaches to biological rhythms in *Drosophila*. Methods Enzymol 393:61–185.

Hardin PE. 2004. Transcription regulation within the circadian clock: the E-box and beyond. J Biol Rhythms 19:348–360.

Helfrich-Förster C. 1998. Robust circadian rhythmicity of *Drosophila melanogaster* requires the presence of lateral neurons: a brain-behavioral study of *disconnected* mutants. J Comp Physiol A 182:435–453.

Helfrich-Förster C. 2003. The neuroarchitecture of the circadian clock in the brain of *Drosophila melanogaster*. Microsc Res Techn 62:94–102.

Helfrich-Förster C. 2005. Techniques that revealed the network of the circadian clock of *Drosophila*. Methods Enzymol 393:439–451.

Helfrich-Förster C, Winter C, Hofbauer A, Hall JC, Stanewsky R. 2001. The circadian clock of fruit flies is blind after elimination of all known photoreceptors. Neuron 30:249–261.

Kaneko M, Hall JC. 2000. Neuroanatomy of cells expressing clock genes in *Drosophila*: transgeneic manipulation of the *period* and *timeless* genes to mark the perikarya of circadian pacemaker neurons and their projections. J Comp Neurol 422:66–94.

Klarsfeld A, Malpel S, Michard-Vanhée C, Picot M, Chélot E, Rouyer F. 2004. Novel features of cryptochrome-mediated photoreception in the brain circadian clock of *Drosophila*. J Neurosci 24:1468–1477.

Leak RK, Moore RY. 2000. Topographic organization of suprachiasmatic nucleus projection neurons. J Comp Neurol 433:312–334.

Lin Y, Stormo GD, Taghert PH. 2004. The neuropeptide pigment-dispersing factor coordinates pacemaker interactions in the *Drosophila* circadian system. J Neurosci 24:7951–7957.

Lindsley DL, Zimm GG. 1992. Genetic variations of *Drosophila melanogaster*. San Diego: Academic Press.

Liu X, Zwiebel LJ, Hinton D, Benzer S, Hall JC, Rosbash M. 1992. The period gene encodes a predominantly nuclear protein in adult *Drosophila*. J Neurosci 12:2735–2744.

Moses K, Rubin GM. 1991. Glass encodes a site-specific DNA-binding protein that is regulated in response to positional signals in the developing *Drosophila* eye. Genes Dev 5:583–593.

Moses K, Ellis MC, Rubin RM. 1989. The glass gene encodes a zinc-finger protein required by Drosophila photoreceptor cells. Nature 340:531–536.

Nitabach MN, Blau J, Holmes TC. 2002. Electrical silencing of Drosophila pacemaker neurons stops the free-running circadian clock. Cell 109: 485–495.

O'Neill EM, Rebay I, Tijan R, Rubin GM. 1994. The activities of two Ets-related transcription factors required for *Drosophila* eye development are modulated by the Ras/MAPK pathway. Cell 78:137–147.

Park JH, Helfrich-Forster C, Lee G, Liu L, Rosbash M, Hall JC. 2000. Differential regulation of circadian pacemaker output by separate clock genes in Drosophila. Proc Natl Acad Sci U S A 97:3608–3613.

Peng Y, Stoleru D, Levine JD, Hall JC, Rosbash M. 2003. *Drosophila*

free-running rhythms rquire intercellular communication. Pub Lib Sci Biol 1:32–40.

Renn SCP, Park JH, Rosbash M, Hall JC, Taghert PH. 1999. A *pdf* neuropeptide gene mutation and ablation of PDF neurons each cause severe abnormalities of behavioral circadian rhythms in *Drosophila*. Cell 99:971–802.

Samson ML, Lisbin MJ, White K. 1995. Two distinct temperature-sensitive alleles at the elav locus of *Drosophila* are suppressed nonsense mutations of the same tryptophan codon. Genetics 141:1101–1111.

Schneider LE, Roberts MS, Taghert PH. 1993. Cell type-specific transcriptional regulation of the *Drosophila FMRFamide* neuropeptide gene. Neuron 10:279–291.

Schöning JC, Staiger D. 2005. At the pulse of time: protein interactions determine the pace of circadian clocks. FEBS Lett 579:3246–3252.

Sepp KJ, Auld VJ. 1999. Conversion of lacZ enhancer trap lines to GAL4 lines using targeted transposition in *Drosophila melanogaster*. Genetics 151:1093–1101.

Shafer OT, Rosbash M, Truman JW. 2002. Sequential nuclear accumulation of the clock proteins Period and Timeless in the pacemaker neurons of *Drosophila melanogaster*. J Neurosci 22:5946–5954.

Stoleru D, Ping Y, Agosto J, Rosbash M. 2004. Coupled oscillators control morning and evening locomotor behavior in *Drosophila*. Nature 431: 862–868.

Suh GS, Wong AM, Hergarden AC, Wang JW, Simon AF, Benzer S, Axel R, Anderson DJ. 2004. A single population of olfactory sensory neurons mediates an innate avoidance behaviour in *Drosophila*. Nature 431: 854–8599.

Taghert PH, Lin Y. 2005. Tick-talk: the cellular and molecular biology of *Drosophila* circadian rhythms. In: Gilbert LI, Iatrou K, Gill SS, editors. Comprehensive molecular insect science. Amsterdam: Elsevier. p 357–395.

Taghert PH, Hewes RS, Park JH, O'Brien MA, Han M, Peck ME. 2001. Multiple amidated neuropeptides are required for normal circadian rhythmicity in *Drosophila*. J Neurosci 21:6673–6686.

Veleri S, Brandes C, Helfrich-Förster C, Hall JC, Stanewsky R. 2003. A self-sustaining, light-entrainable circadian oscillator in the *Drosophila* brain. Curr Biol 13:1758–1767.

Verleyen P, Baggerman G, Wiehart W, Schoeters E, Van Lommel A, De Loof A, Schoofs L. 2004. Expression of a novel neuropeptide, NVGT-LARDFQLPIPNamide, in the larval and adult brain of *Drosophila melanogaster*. J Neurochem 88:311–319.

Yang Z, Sehgal A. 2001. Role of molecular oscillations in generating behavioral rhythms in *Drosophila*. Neuron 29:453–467.

Yoshii T, Heshiki Y, Ibuki-Ishibashi T, Matsumoto A, Tanimura T, Tomioka K. 2005. Temperature cycles drive *Drosophila* circadian oscillation in constant light that otherwise induces behavioural arrhythmicity. Eur J Neurosci 22:1176–1184.

Zhao J, Kilman VL, Keegan KP, Peng Y, Emery P, Rosbash M, Allada R. 2003. *Drosophila Clock* can generate ectopic circadian clocks. Cell 13:755–766.